Electrochimica Acta 247 (2017) 600–609

Contents lists available at ScienceDirect

Electrochimica Acta

journal homepage: www.elsevier.com/locate/electacta

The effect of electrolyte additives on electrochemical performance of silicon/mesoporous carbon (Si/MC) for anode materials for lithium-ion batteries

Arlavinda Rezqita[a,b,*], Markus Sauer[c], Annette Foelske[c], Hermann Kronberger[b], Atanaska Trifonova[a]

[a] AIT Austrian Institute of Technology GmbH, Center for Low-Emission Transport, 1210 Vienna, Austria
[b] Vienna University of Technology, Institute of Chemical Technologies and Analytics, 1060 Vienna, Austria
[c] Vienna University of Technology, Analytical Instrumentation Center, 1060 Vienna, Austria

ARTICLE INFO

Article history:
Received 15 December 2016
Received in revised form 19 June 2017
Accepted 21 June 2017
Available online 29 June 2017

Keywords:
Li-ion batteries
electrolyte additives
silicon/carbon anodes
SEI layer
initial capacity loss
XPS analysis

ABSTRACT

We investigated the effect of different electrolyte additives such as vinyl carbonate (VC), succinic anhydride (SA), and lithium bis(oxalato)borate (LiBOB) on the chemical composition of Solid Electrolyte Interphase (SEI) layer and the electrochemical performance of Si/MC electrodes. The electrochemical behavior of the Si/MC electrodes was evaluated by galvanostatic charge/discharge and rate capability tests. It was found that various electrolyte compositions result in the formation and the resulting properties of the SEI of the electrodes with different compounds. From X-ray Photoelectron Spectroscopy (XPS) analysis, the electrodes cycled in SA- and LiBOB-containing electrolytes show a higher amount of lithium carbonates and a thicker SEI layer than those in standard and VC-containing electrolyte. The electrode with VC 5w% shows an excellent reversible capacity of ~1100 mAh g^{-1} up to 100 charge-discharge cycles.

1. Introduction

New applications, such as in electrical vehicles and renewable energy storages increase the requirements on the electrochemical performances of Li-ion cells. Improvements in battery life require optimization of the electrode structure as well as an appropriate choice of electrolyte. Si offers the highest theoretical specific capacity (4200 mAh g^{-1}), a low lithiation potential (~0.2 V vs. Li/Li^+), and a high abundancy on earth. The main shortcoming of Si anodes is the volume change (~400%) during lithium alloying/dealloying and the high irreversible capacity losses during the first charge-discharge cycle. It causes progressive pulverization and electric contact loss leading to capacity fading [1]. Although the volume expansion can be minimized by the use of Si nano-powders and the conductivity problem can be overcome by conductive additive, some issues related to the solid electrolyte interphase (SEI) are still present. The chemical structure and morphology of SEI influence safety, cycle life, side reactions, and durability of Li-ion batteries [2–4]. We remind the reader that SEI growth occurs at the negative electrode because standard electrolytes are not stable at the operating potential of the electrode during charging. This continous formation of SEI increases the electrical resistance of the electrode and hinders Li-ion diffusion to the active anode material. In addition, SEI layer can trap some amount of Li and cause initial capacity loss [5]. The most prevalent strategy for dealing with this initial capacity loss associated with continuous electrolyte decomposition is the use of electrolyte additives. Additives for anodes are expected to facilitate the formation of SEI layer on the surface of the electrodes at a higher potential compared to pure carbonate electrolytes. Vinyl carbonate (VC) [6–12], fluoroethylene carbonate (FEC) [6,7,13], lithium bis(oxalato)borate (LiBOB) [9,14], lithium difluorooxalato-borate (LiDFOB) [6], succinic anhydride (SA) [15,16], and tris (pentafluorophenyl)borane (TPFPB) [17], have been studied as electrolyte additives for Si anodes. XPS studies show that the addition of VC in electrolyte forms poly(VC) on the electrode surface which makes SEI denser and more stretchable [9]. However, excess of VC can increase the ohmic resistance and results in low cycling efficiency and high self discharge rate. For this reason, adjusting amount of added VC is necessary. The

* Corresponding author at: AIT Austrian Institute of Technology GmbH, Center for Low-Emission Transport, 1210 Vienna, Austria. Tel.: +436804005515; fax.: +43505506595.
E-mail address: arlavinda.rezqita@gmail.com (A. Rezqita).

http://dx.doi.org/10.1016/j.electacta.2017.06.128

addition of LiBOB has shown to generate higher concentration of oxalates and $Li_xPF_yO_z$, but lower LiF providing a modest improvement in cycling performance on Si thin film electrodes [6]. Han et al. showed that the presence of SA can cultivate a higher content of hydrocarbon and Li_2CO_3 on the Si thin film [15]. Li et al. showed that the use of SA could improve the electrochemical behavior of Si/C nanofiber by preventing the decomposition of $LiPF_6$ [16].

Although the beneficial role of those aforementioned electrolyte additives on the Si electrode/electrolyte interfaces has been demonstrated, there are no comparative studies on the effects of LiBOB, SA, and VC for Si/MC electrodes. In addition, most previous studies regarding these electrolyte additives focus on Si thin film electrodes which might behave differently from Si nanoparticles-based anodes. In this paper, we aim to investigate the effect of VC, SA, and LiBOB on the chemical composition of SEI layer and the electrochemical performance of the Si/MC electrodes. In addition, we investigate different concentrations of VC on the electrochemical performance of Si/MC anodes. Various characterization tools such as galvanostatic cycling, X-ray photoelectron spectroscopy (XPS), Scanning Electron Microscopy (SEM), were used in this work.

2. Experimental

2.1. Electrode preparation

The electrodes were prepared from Si/MC composites (75 wt%), Super C45 (15 wt%, Timcal), polyacrylic acid (PAA, 10 wt%, Sigma Aldrich) and dissolved in N-methyl-2-2pyrrolidinone (NMP, Sigma Aldrich). The Si/MC composites were prepared with the same method which is reported in a previous study [18]. The content of Si in the Si/C composite was 12 wt%. The slurry was coated onto a copper foil and dried at room temperature and subsequently at 60 °C for 2 h and 120 °C for 4 h under vacuum at a pressure of 0.09 MPa. The dried layer was rolled between two stainless steel rolls at 120 °C to reduce porosity. Thereafter, the electrodes with a diameter of 15 mm were dried at 120 °C overnight under vacuum. The electrode loading mass was determined to be 0.95 mg cm^{-2} with the thickness of 0.04 mm.

2.2. Electrochemical measurements

Electrochemical characterization was performed in 2032-type coin cells (XL Labwares PTe Ltd). Li foil was used as a counter electrode. The standard electrolyte (100 μL) used was 1 M $LiPF_6$ in 1:1 vol mixture ethylene carbonate (EC) and dimethyl carbonate (DMC) without additive. The electrolyte additives used in this study were VC, SA, LiBOB (all additives were purchased from Sigma Aldrich and used as received). The electrolyte compositions are shown in Tables 1 and 2. Fig. 1 shows the chemical structure of the additives used in this study. Three layers of polypropylene microporous membrane (thickness: 25 μm) manufactured by Freunberger group were used as separator. The charge/discharge tests were conducted using constant current-constant voltage (CCCV) mode. For the first cycle, the electrodes were first lithiated at a current of C/20 and then held at 50 mV until the current decayed to a value of 10% of the current used during galvanostatic charge for respective C-rate. Then the electrodes were delithiated at C/20 until a 1 V cut off was reached. Afterwards, they were lithiated/delithiated at a C/10 rate. For the rate capability test, a series of different current density of C/20, C/10, C/3, C/2, 1C, 2C has been performed with constant current mode. The C-rate was calculated based on the theoretical capacity of Si and the theoretical capacity of mesoporous carbon. It should be noted that the study was performed using Li-Si/MC cells, thus, the term of discharge process here refers to the lithiation process. Coulombic efficiency (CE) was determined by calculating the ratio of discharge capacity to charge capacity for every cycle. Capacity retention (CR) in this work was calculated by dividing the discharge capacity of the n^{th} cycle by the initial discharge capacity. All electrochemical measurements were performed in a Maccor Series 4000 battery tester at room temperature.

Table 1
Electrolyte compositions for investigation of different electrolyte additives.

Standard	1 M $LiPF_6$ in EC: DMC (1:1)
VC 5 wt%	1 M $LiPF_6$ in EC: DMC (1:1) + 5 wt% VC
SA 5 wt%	1 M $LiPF_6$ in EC: DMC (1:1) + 5 wt% SA
LiBOB 5 wt%	1 M $LiPF_6$ in EC: DMC (1:1) + 5 wt% LiBOB

Table 2
Electrolyte compositions for investigation of different concentrations of VC.

Standard	1 M $LiPF_6$ in EC: DMC (1:1)
VC 3 wt%	1 M $LiPF_6$ in EC: DMC (1:1) + 3 wt% VC
VC 5 wt%	1 M $LiPF_6$ in EC: DMC (1:1) + 5 wt% VC
VC 10 wt%	1 M $LiPF_6$ in EC: DMC (1:1) + 10 wt% VC

2.3. Ex-situ XPS and SEM analysis

For ex-situ analysis, the electrodes were extracted from the coin cells after discharged state in an Argon-filled glove box (MBRAUN). The electrodes were washed gently in extra pure DMC four times to remove Li salts and dried overnight at room temperature. For XPS analysis, the samples were mounted onto a sample holder inside the glove box, and subsequently, transferred into a desiccator under argon atmosphere to the XPS system where the samples were transferred into the ultra-high vacuum chamber. The exposure time of the samples to air was limited to less than 1 minute. XPS analysis was carried out using a SPECS XPS-spectrometer equipped with a monochromatic Al-Kα source (1486.6 eV at 88 W, spot diameter 500 μm) and a hemispherical WAL-150 analyser. Survey spectra and narrow scans were recorded using pass energies of 100 eV and 30 eV with energy resolutions of 500 meV and 50 meV, respectively. The pressure was kept lower than 2×10^{-9} mbar during measurements. CASA-XPS software was used for data analysis. Quantification of the detected elements was carried out from survey scans using transmission corrections, Scofield sensitivity factors and Tougaard backgrounds [19,20]. The accuracy of XPS measurements was better than ±10% of the determined values. SEM analysis was conducted by FEI/Philips XL-30 Field Emission ESEM.

3. Results and discussion

3.1. Electrochemical performance

3.1.1. Electrochemical performance of Si/MC electrodes with different electrolyte additives

The discharge capacity versus cycle number of Si/MC electrodes with different electrolyte additives is presented in Fig. 2a. The electrode with standard electrolyte shows an initial discharge capacity of 3944 mAh g^{-1} which decreases to 682 mAh g^{-1} after 100 cycles. The decrease in capacity at the first several cycles is attributed to the decomposition of electrolyte and the formation of SEI. On the other hand, Si/MC electrodes with electrolyte additives deliver reversible capacities higher than the one with standard electrolyte. The electrode with SA 5 wt% shows a decreasing discharge capacity from 3796 mAh g^{-1} to 807 mAh g^{-1} after 100 cycles. With the addition of LiBOB 5 wt%, the electrode exhibits a higher initial capacity loss of 2461 $mAhg^{-1}$ (58.2% of initial

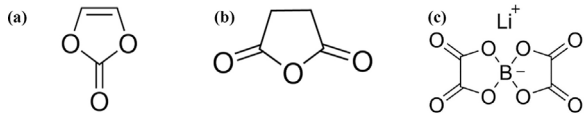

Fig. 1. Chemical structure of chemical additives: vinyl carbonate (a), succinic anydride (SA) (b), and lithium bi(oxalato)borate (LiBOB) (c) used in this work.

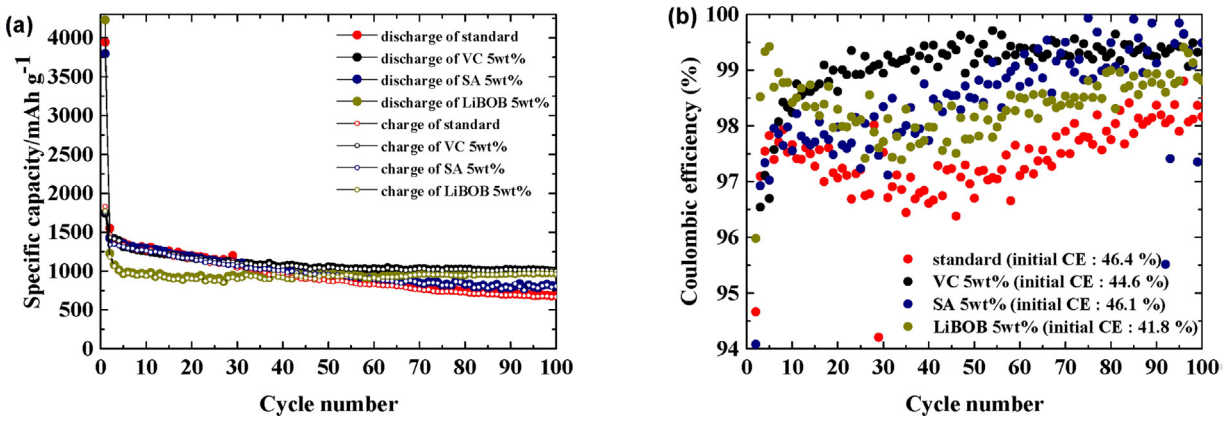

Fig. 2. Specific capacity (a) and coulombic efficiency (b) vs cycle number of Si/MC electrodes with different electrolyte additives under charge/discharge cycles from 1 to 0.005 V with a charge/discharge current of C/10.

discharge capacity). However, it shows a stable discharge capacity after 20 cycles (970 mAh g^{-1}). This is in good agreement with a previous study in which it was proposed that the decomposition reaction of LiBOB was faster with respect to $LiPF_6$ and inhibited the continuous reactions of lithiated Si with the electrolyte [21]. Thus, LiBOB can be supposed to be more effective in forming a stable SEI layer. Compared with other electrodes, the electrode with VC 5 wt% has a more stable performance with a reversible capacity of 1100 mAh g^{-1} after 20 cycles which remains stable in the subsequent cycles. This distinct electrochemical performance may be related to the particular composition of SEI which is later discussed based on XPS analysis.

To verify the irreversible capacity loss of the electrodes, CE profiles were compared and are shown in Fig. 2b. The electrode with standard electrolyte exhibits the initial CE of 46.4% and 98.17% after 100 cycles. The electrodes with SA and LiBOB reach the stable CE of over 99% after 80 cycles, meanwhile, the one with the VC additive shows CE over 99% just after 20 cycles. It can be seen that with LiBOB, the discharge capacity decreases, but the CE increases. This phenomenon may be explained by a thickening of the SEI layer which increases the internal resistance of the cell. Electrochemical performance of Si/MC electrodes with different electrolytes at 1st and 20th cycles can be seen in Table 3.

The stability of Si/MC electrodes was further assessed by a rate capability test. Fig. 3 shows the specific capacity vs. cycle number at various C-rates. The specific capacity gradually decreases with increasing C-rate from C/20 to 2C and increases again when the C-rate is lowered. Upon cycling, the electrode with the standard electrolyte shows a poor rate capability. At C/10, the average discharge capacity of the electrode working with the standard electrolyte is 1375 mAh g^{-1} at the 20th cycle and decreases to 816 mAh g^{-1} at the 100th cycle. On the other hand, the addition of VC results in a higher rate capability than those with SA and LiBOB. The electrode with VC shows 1332 mAh g^{-1} at the 20th cycle and maintains at 1050 mAh g^{-1} at the 100th cycle.

The CE at various C-rate was calculated and the profiles are depicted in Fig. 3b. After 20 cycles, all electrodes reach high coulombic efficiencies of more than 96%. After 110 cycles at C/10, the CE of the electrodes with standard electrolyte, VC, SA, and LiBOB reaches 97.3%, 99.3%, 98.9%, and 98.5%, respectively. These results confirm that the addition of VC 5 wt% improves the electrochemical performance more than those with other electrolyte additives. The variation of CE values can be due to the continuous changes of Si nanoparticles which cause some fluctuation in ionic and electric conductivities from cycle to cycle. Thus, the varying arrangement of Si nanoparticles can also cause fluctuations in the capacities by casual charge retention or release leading to a “virtual” CE greater than 100%. In other words, some residual Li stored in the previous cycles can be released additionally in the following cycles. This noticeable phenomenon was also observed in the Si nanoparticles wrapped by carbon shell by Hwang et al. [22].

In order to investigate the electrochemical behavior in more detail, potential vs. specific capacity profile and differential capacity (dQ/dV) profile have been performed and presented in Fig. 4. The phase transitions on the potential vs. specific capacity profile (Fig. 4a) can be identified more clearly on dQ/dV vs. potential plots.

Table 3
Electrochemical performance of Si/MC electrodes with different electrolytes at the 1st and 20th cycles.

Electrolyte additive	CE at 1st cycle (%)	Charge capacity at 20th cycle (mAh g^{-1})	Discharge capacity at 20th cycle (mAh g^{-1})	CR at 20th cycle (%)	CE at 20th cycle (%)
standard	46.4	1163	1198	30.4	97.1
VC 5 wt%	44.6	1177	1193	30.5	98.6
SA 5 wt%	46.1	1165	1189	31.3	97.9
LiBOB 5 wt%	41.8	904	919	21.7	98.3

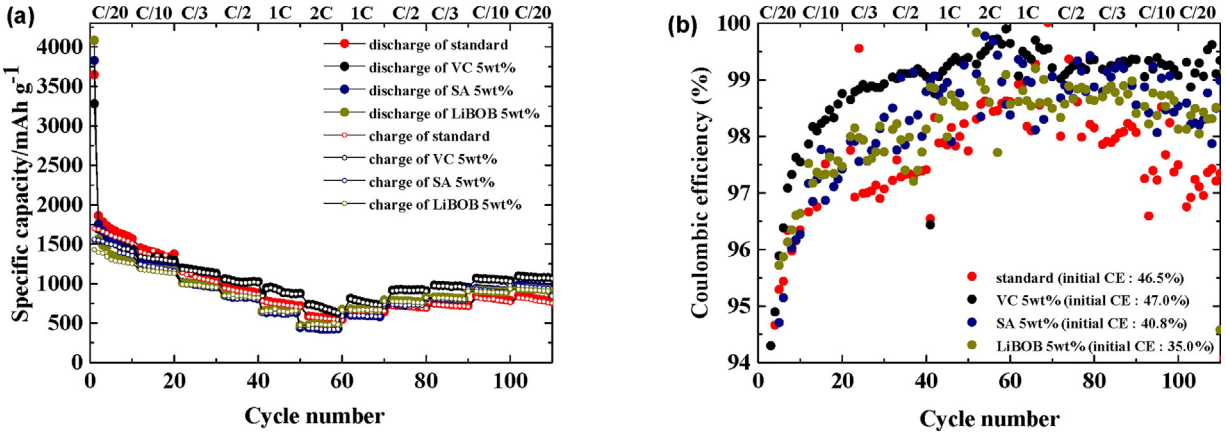

Fig. 3. Rate capability (a) and coulombic efficiency (b) vs. cycle number of Si/MC electrode with different electrolytes at various C-rate (C/20, C/10, C/3, C/2, 1C, 2C) from 1 to 0.005 V vs Li/Li^+.

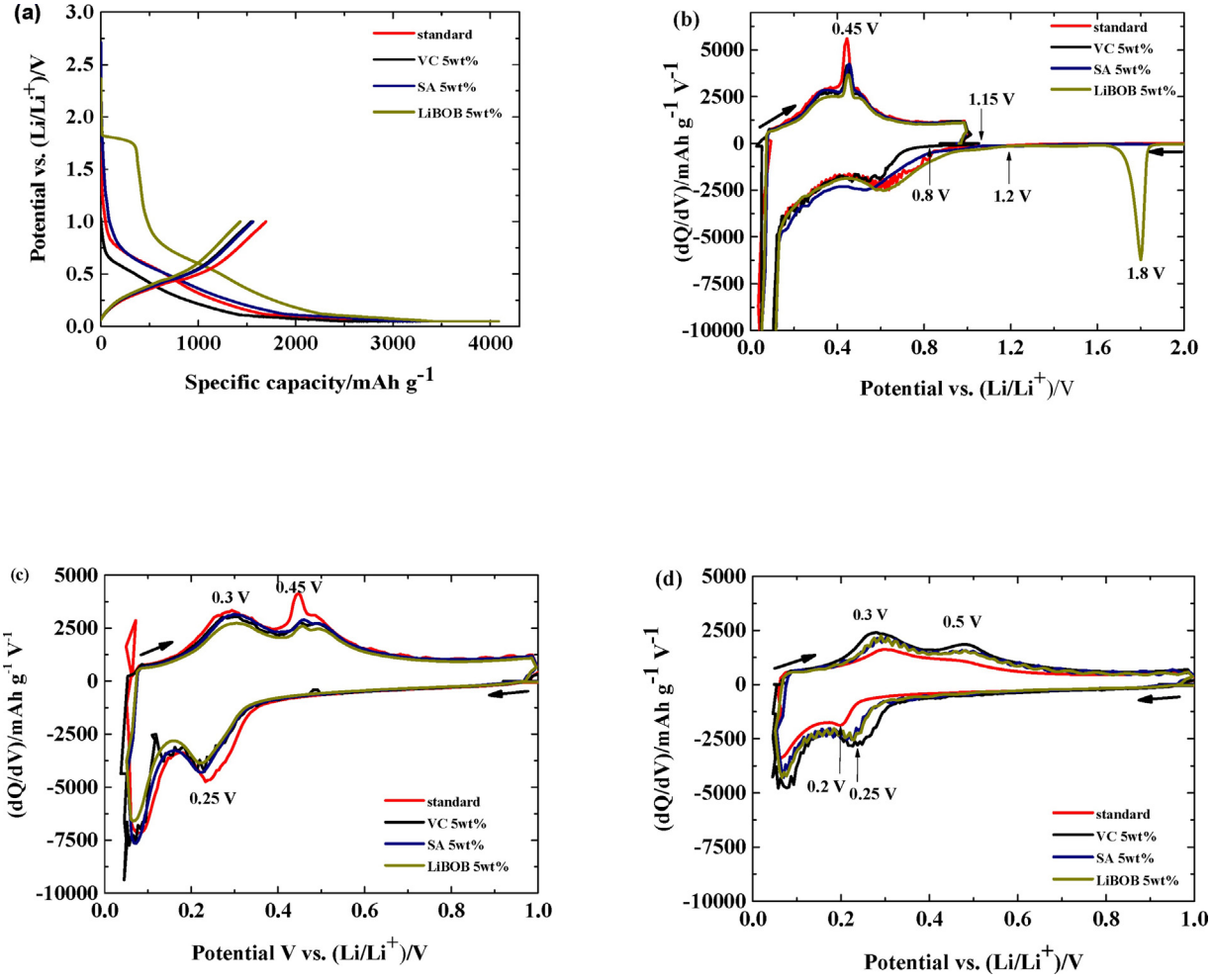

Fig. 4. Potential vs. capacity profile (a) and differential capacity (dQ/dV) vs. potential plots of Si/MC electrodes with different electrolytes at 1st (b), 2nd (c), and 110th (d) cycle from 1 to 0.005 V vs Li/Li^+.

The peaks at 1st cycle (Fig. 4b) show the potential at which the electrolyte is initially reduced. The reduction of the standard electrolyte starts at 1.0 V vs. Li/Li^+ and shows a cathodic maximum at 0.6 V vs Li/Li^+. This reduction starts at a different potential with SA (1.15 V vs Li/Li^+) and LiBOB (1.2 V vs. Li/Li^+). With VC as an additive, the starting potential is slightly shifted to a lower value (0.8 V vs. Li/Li^+). This indicates a higher overpotential which is attributed to increased resistance in the SEI [23]. For the LiBOB containing electrolyte, additional reduction peak appears at a much more positive potential of 1.8 V vs. Li/Li^+. A previous study demonstrated that the reduction of the BOB-anion to oxalate occurred at a high potential (> 1 V vs. Li/Li^+) on the graphite anode

[24]. This reduction may explain why the electrode cycled in LiBOB-containing electrolyte exhibits the highest initial charge loss (2461 $mAhg^{-1}$ at the first cycle) compared to those cycled in the other electrolytes. The broad cathodic peak at ~0.6 V vs Li/Li^+ during the 1st cycle (Fig. 4b) which disappears on the 2nd and the 110th cycles (Fig. 4c&d) is attributed to the electrolyte decomposition and SEI formation. In Fig. 4b&c, the anodic peak at 0.45 V vs Li/Li^+ is easily identifiable by dQ/dV, especially for the Si/MC electrode with standard electrolyte. According to Obrovac et al. the anodic peak at ~0.45 V vs Li/Li^+ is the dQ/dV signature of $Li_{15}Si_4$ phase – delithiation [25]. The presence of $Li_{15}Si_4$ was associated with capacity fading due to inhomogeneous volume changes. Chevrier et al. suggested that the magnitude and the sharpness of the peak could be a measure of the $Li_{15}Si_4$ phase at full lithiation [26].

The dQ/dV plots for the 2nd and 110th cycles are different from the 1st cycle. During the 2nd cycle (Fig. 4c), all the dQ/dV plots show two reduction peaks at ~0.25 V and 0.05 V vs. Li/Li^+. According to [25], these peaks correspond to the stepwise lithium insertion into amorphous silicon forming amorphous Li_xSi ((α-Si + x'Li → α-Li_x'Si) and (α-Li_x'Si + x"Li → α-$Li_{(x'+x")}$Si)). At the 110th cycle after applying a high C-rate (Fig. 4d), the intensity of the peaks at 0.25 V at lithiation and 0.5 V at delithiation decreases significantly. This indicates the $Li_{15}Si_4$ phase gradually decomposing with cycling. All electrodes show the decreasing intensity of the peaks at 0.25 V and 0.1 V during lithiation which means less insertion of lithium into amorphous silicon. It can be noted that the electrode with VC 5 wt% shows a slight difference of peaks to a higher potential for lithiation (0.25 V vs Li/Li^+) compared to the standard electrode (0.2 V vs Li/Li^+) which we attribute to different reaction kinetics. In addition, compared to the 2nd cycle, the electrodes at the 110th cycle show significant peak shifts towards lower voltage for the lithiation and towards higher voltage for the process of delithiation which can be assigned to increasing overpotential over cycling. This phenomenon was also investigated by Zhang et al. [27]. Contrary to the electrode with standard electrolyte which shows the highest overpotential, the electrode with 5 wt% VC exhibits the lowest overpotential.

3.1.2. Electrochemical performance of Si/MC electrodes with different concentrations of VC

From the results presented above, we conclude that compared to the additives LiBOB and SA, VC improved the electrochemical performance of Si/MC electrodes more effectively. As excess in VC can increase the electrodes' ohmic resistance, the effective amount of VC is worthy of further investigation. To the best of our knowledge, previous studies on VC additives mostly focused on Si thin film-based and graphite anodes. There is no study about the effect of different concentrations of VC on Si/C-based composites so far.

Fig. 5a shows specific capacity vs. cycle number profiles of the Si/MC electrodes with different amounts of VC. It is worth noting that increasing the amount of VC does not necessarily increase the electrodes' specific capacity. In fact, the electrode with VC 5 wt% shows the greatest electrochemical performance (with a capacity retention of 30.5% at 20th cycle). The CE profile (Fig. 5b) shows that electrodes with VC additives regardless of the concentrations exhibit a higher CE than the one with standard electrolyte. The electrode with VC 10 wt% reaches ≥99% after 5 cycles. The electrochemical performance of Si/MC electrodes with different concentrations of VC at 1st and 20th cycle is summarized in Table 4.

Rate capability tests for the Si/MC electrodes with different concentrations of VC were performed and are depicted in Fig. 6a. At C/10 at the 110th cycle, the electrode with VC 3 wt% exhibits ~750 $mAh\,g^{-1}$, while the electrode with VC 10 wt% shows 953 $mAh\,g^{-1}$ at the 110th cycle. Compared to the electrode with VC 5 wt% (1054 $mAh\,g^{-1}$ for the 110th cycle), the electrodes with 3 wt% and 10 wt% of VC show less stable performance. These results confirm those of the charge-discharge test mentioned above, and show that electrochemical performance of the electrolyte with 5 wt% VC is better than at other concentrations, i.e. at 3 wt% and

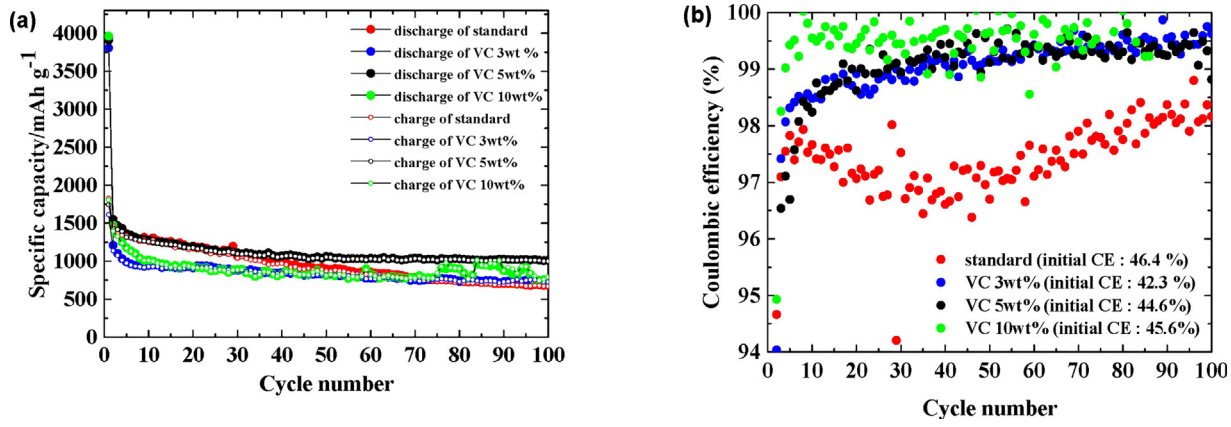

Fig. 5. Specific capacity (a) and coulombic efficiency (b) vs cycle number of Si/MC electrodes with different amounts of VC under charge/discharge cycles with a charge/discharge current of C/10 from 1 to 0.005 V vs Li/Li^+.

Table 4
Electrochemical performance of Si/MC electrodes with different concentrations of VC at the 1 st and 20th cycle.

Electrolyte additive	CE at 1st cycle (%)	Charge capacity at 20th cycle ($mAh\,g^{-1}$)	Discharge capacity at 20th cycle ($mAh\,g^{-1}$)	CR at 20th cycle (%)	CE at 20th cycle (%)
standard	46.4	1163	1198	30.4	97.1
VC 3 wt%	42.3	901	911	23.9	98.9
VC 5 wt%	44.6	1177	1193	30.5	98.6
VC 10 wt%	45.6	918	923	23.2	99.5

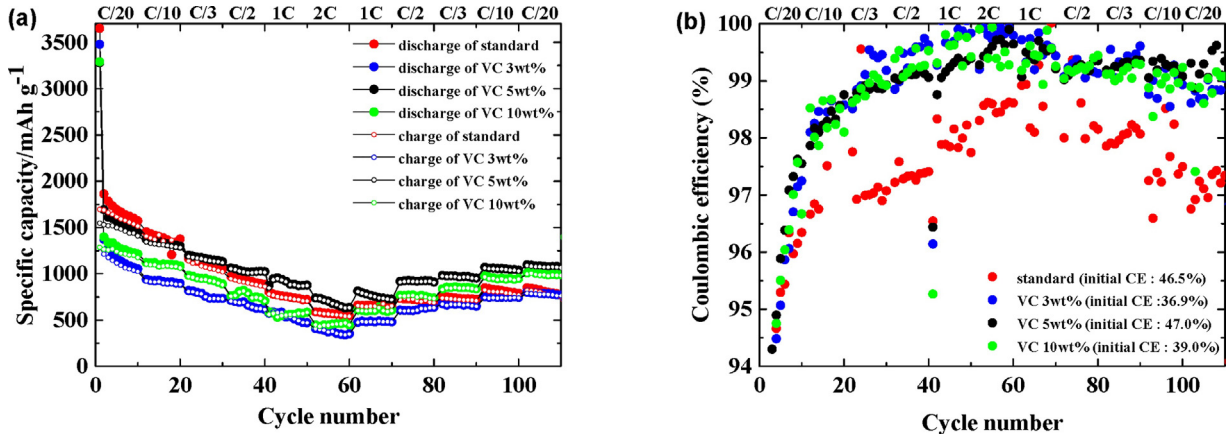

Fig. 6. Rate capability (a) and columbic efficiency (b) vs. cycle number of Si/MC electrode with different concentrations of VC at various C-rates (C/20, C/10, C/3, C/2, 1C, 2C) from 1 to 0.005 V vs Li/Li^+.

10 wt%. To be noted also from Fig. 6b, we can see that the electrodes with VC additives reach CE values higher than 98% after 20 cycles, while the one with standard electrolyte shows CE below 98% upon cycling.

The potential vs. specific capacity profiles at the 1st cycle and the differential capacity (dQ/dV) vs. potential plots of Si/MC electrodes using different concentrations of VC can be seen in Fig. 7. The (dQ/dV) vs. potential plots (Fig. 7b) shows that the electrode with 3 wt% and 5 wt% of VC show initial decomposition from 0.8 V vs. Li/Li^+; that is lower than in those with the standard electrolyte and VC 10 wt% (0.9 V vs. Li/Li^+). From the 2nd cycle (Fig. 7c) to the 110th cycle (Fig. 7d), the Si/MC electrode with standard electrolyte shows a shift of the reduction peak potential from 0.25 V to 0.2 V vs. Li/Li^+. On the other hand, the electrodes with VC additives show no reduction potential shift. Their reduction peaks remain at 0.25 V vs Li/Li^+. At the 110th cycle,

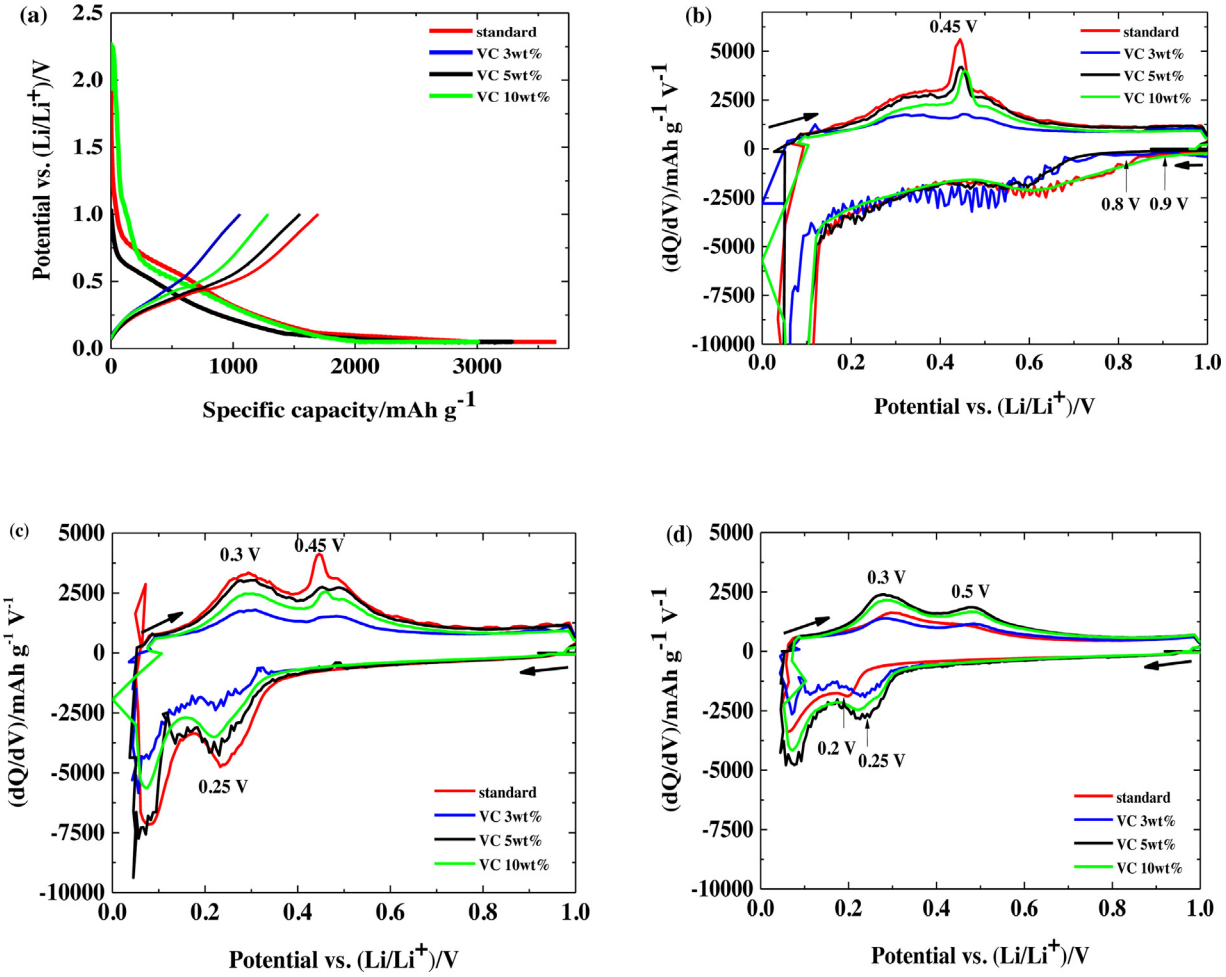

Fig. 7. Potential vs. capacity profile (a) and differential capacity (dQ/dV) vs. potential plots of Si/MC electrodes with different concentrations of VC at 1st (b), 2nd (c), and 110th (d) cycle from 1 to 0.005 V vs Li/Li^+.

the peaks are less pronounced for the electrode with standard electrolyte and most pronounced for the one with VC 5 wt%. Hausbrand et al. reviewed that the degradation can be characterized by irreversible capacity loss, voltage loss, and increase in cell impedance [28]. Thus, we can conclude that the addition of 5 wt% VC delivered the greatest electrochemical performance. As for the reasons, we assume that too low a concentration of VC (3 wt%) does not optimally improve the electrochemical performance of Si/MC electrodes because it is insufficient to build a stable SEI layer. On the other hand, too high a concentration of VC (10 wt%) can increase the content of the polymerized VC on the SEI layer, which in turn leads to decreasing ionic conductivity.

3.2. Surface analysis of SEI modification with different electrolyte additives

3.2.1. SEM analysis

SEM images of Si/MC electrodes with different electrolytes taken after 20 cycles are depicted in Fig. 8. The electrode with standard electrolyte shows agglomerate particles, some of white color, and cracks. A similar morphology can be seen for the electrodes with the electrolyte additives. The white color on the surfaces can be assigned to deposited Li-salts. This white color is more pronounced on the electrode with LiBOB, which also explains the increased decomposition of electrolyte noted above.

3.2.2. XPS analysis

3.2.2.1. Quantification of the sample contents. XPS analysis was conducted in this work in order to understand in more detail the composition of SEI layers on the Si/MC electrodes after 20 cycles with different electrolytes. Fig. 9 shows the XPS survey spectra with the regions used for quantification of the detected elements for different samples with standard electrolyte, 5 wt% VC, 5 wt% LiBOB and 5 wt% SA in comparison with the pristine electrode. The relative contents (in at%) of the detected elements are depicted in Table 5. On the pristine electrode, apart from C, O, and Si, small amounts of Cu, F, and N presumably originating from the current collector, the electrode material, and the preparation process are detected. Neither Cu nor N could be observed on the cycled electrodes. However, small traces of Si could be found on the standard electrolyte and the VC samples, but not on LiBOB and SA cycled electrodes. The amount of Si on the cycled electrodes is highest on the VC sample, suggesting that the addition of VC leads to the formation of a thinner or less dense SEI layer.

Compared to the electrode cycled in standard electrolyte, those with electrolyte additives show increased C and O concentrations. This can be related to the increasing concentration of Li_2CO_3 and/or deposition of the additives on the SEI, which is confirmed by XPS C1 s spectra (discussed in the next section). The electrodes with standard electrolyte and with VC additive show higher amounts of

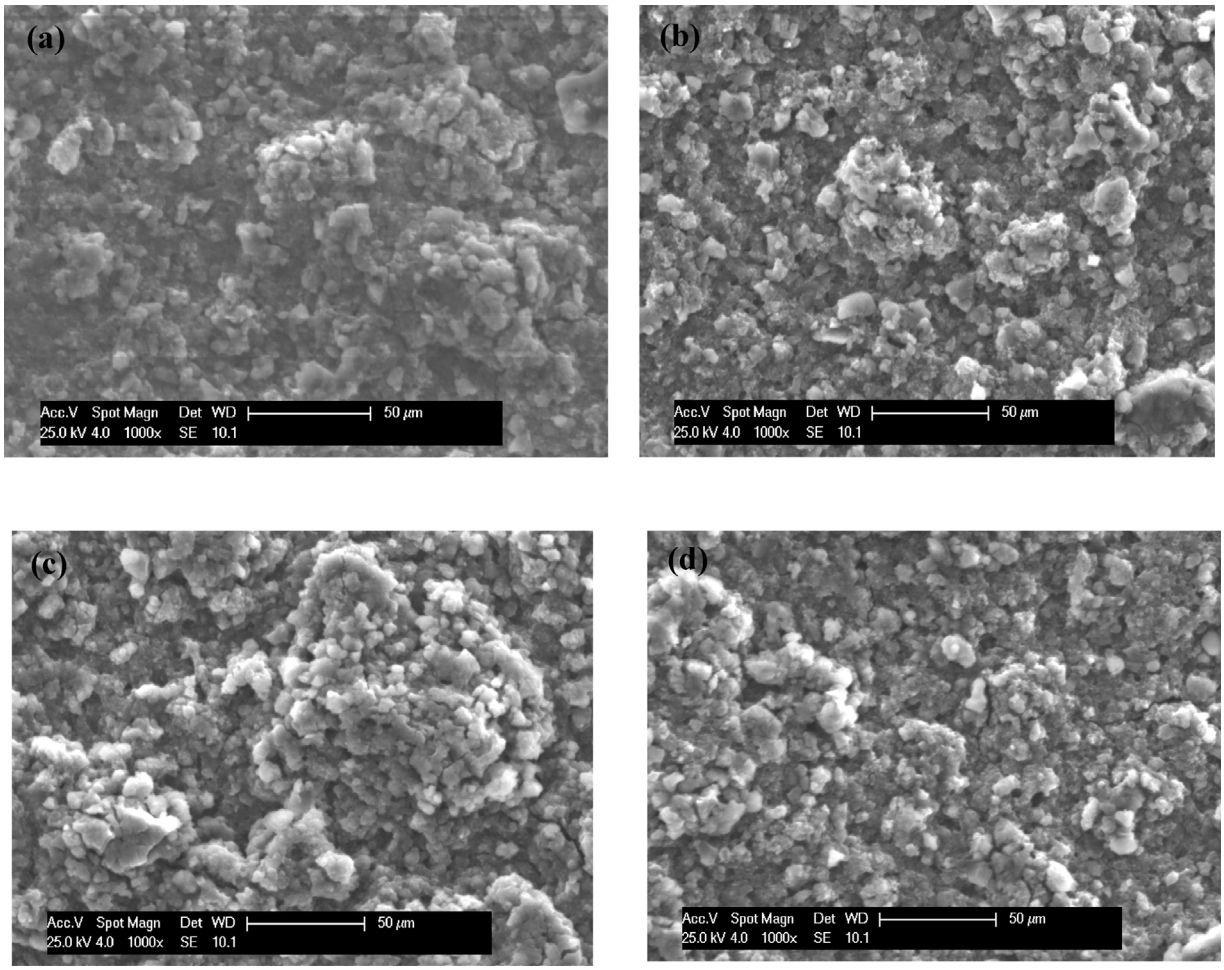

Fig. 8. SEM images of Si/MC electrodes after cycling (20 cycles) with standard electrolyte (a), VC 5 wt% (b), SA 5 wt%, (c), LiBOB 5 wt% (d).

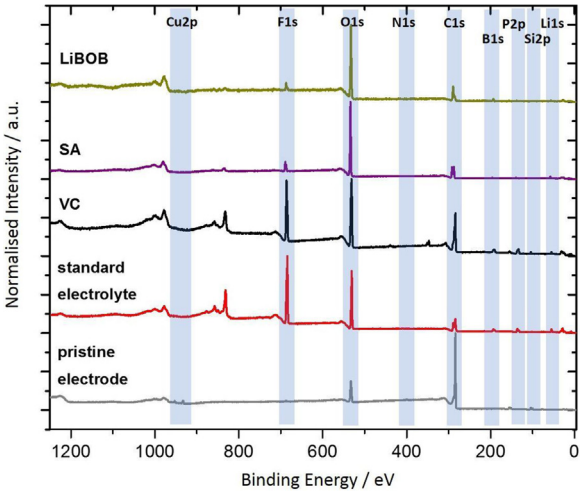

Fig. 9. XPS survey spectra of the cycled Si/MC electrodes with standard electrolyte, VC 5 wt%, SA 5 wt% and LiBOB 5 wt% as well as of the pristine electrode. The light blue areas represent the regions, which have been used for quantification shown in Table 5.

Table 5
Quantitative analysis of the contents of Si/MC samples from XPS analysis.

	Element (in at %)								
Sample	B	C	Cu	F	Li	N	O	P	Si
pristine		81.5	0.4	0.3		0.7	13.2		3.8
standard		20.5		22.7	31.9		21.6	3.0	0.3
VC		38.8		15.4	16.3		24.7	3.6	1.3
SA		29.3		5.1	27.0		37.8	0.8	
LiBOB	7.0	30.4		3.1	17.4		41.6	0.6	

F and P than the samples cycled in LiBOB and SA-containing electrolytes, suggesting a lower amount of $LiPF_6$ on the SEI of the latter samples.

Furthermore, large contributions of boron were found on the electrode cycled in LiBOB-containing electrolyte, indicating that a noticeable amount of this additive is incorporated into the SEI layer.

3.2.2.2. Determination of the components of C, P and F. Fig. 9 shows the XPS C 1s (a), F 1s (b) and P 2p (c) detail spectra of all samples.

Several different species can be assigned to the C 1s spectra (dashed lines in Fig. 10a). The peak at 284.3 eV is attributed to sp^2 like C—C bonds while signals around 285 eV are attributed to C—C/C—H bonds from adventitious carbon. The peak at 286.3 eV is characteristic for C—O. The components at 287.7 eV, 289 eV and 290 eV are attributed to C=O, O—C=O and CO_3 bonds, respectively [29].

The electrodes cycled in standard as well as in VC-containing electrolyte show large amounts of sp^2 carbon from the electrode material and C—C/C—H species confirming the formation of thinner SEI layers in these electrolytes. The difference between VC and standard electrolyte is found in the binding energy range

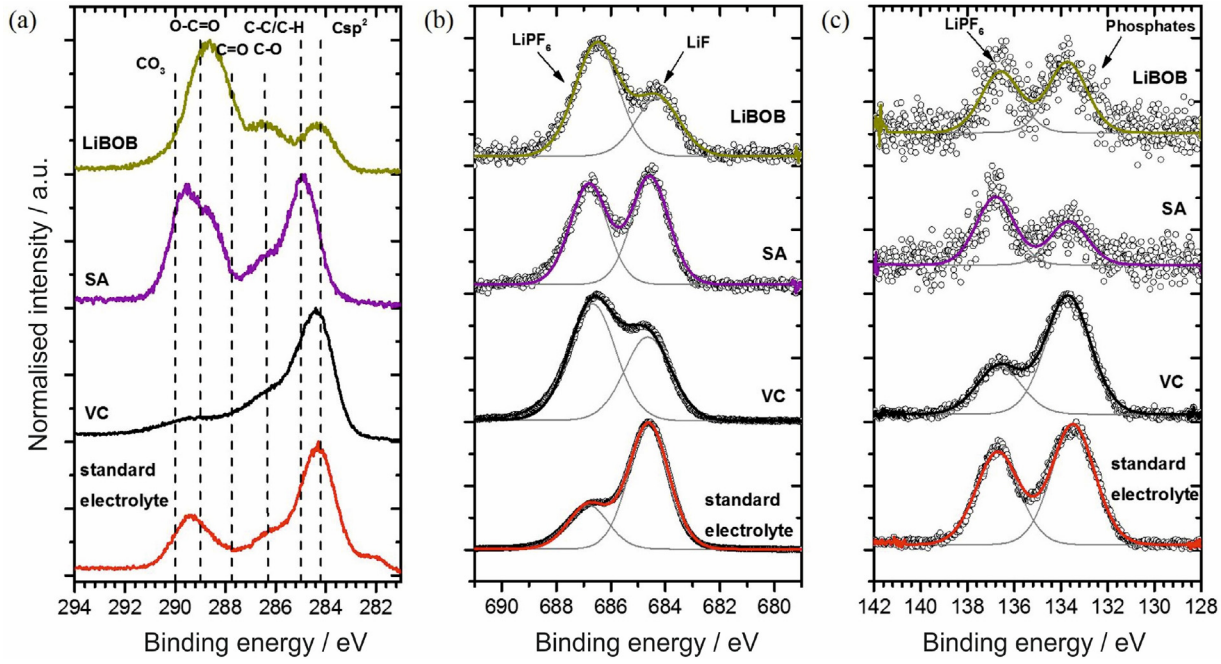

Fig. 10. Normalised C1s (a), F1s (b) and P2p (c) XPS detail spectra of cycled Si/MC electrodes with different electrolytes. Dashed lines in (a) show the positions of different C/O components. Gaussian-Lorentzian line fits in (b) and (c) represent the F and P components as noted on top.

related to O—C=O and CO_3 species. While the use of standard electrolyte leads to formation of lithium carbonates, only small amounts of these compounds can be found for the electrode cycled in VC-containing electrolyte.

In contrast, the samples cycled with SA and LiBOB additives show even higher peak intensities than the standard electrolyte sample in the binding energy range of O—C=O/CO_3. This can be explained by the presence of SA and LiBOB, which both contain these bonding environments, pointing to deposition of these additives on the SEI during cycling as well as the enhanced formation of species like Li_2CO_3 and $ROCO_2Li$ on the electrode surface [30]. This may explain why the electrode with VC 5 wt% shows a higher discharge capacity than those without additive or with other electrolyte additives as fewer Li ions are consumed forming the carbonates.

Li_2CO_3 and $ROCO_2Li$ are the result of the degradation of EC following these reactions:

$$EC + 2e^- + 2Li^+ \rightarrow Li_2CO_3 + CH_2 = CH_2 \quad (1)$$

$$2EC + 2e- + 2Li^+ \rightarrow (CH_2OCO_2Li)_2 + CH_2 = CH_2 \quad (2)$$

The F 1 s and P 2p spectra which enable the investigation of electrolyte decomposition are presented in Fig. 10b&c. The F 1 s spectra (Fig. 10b) show two peaks at 686.8 eV and 684.6 eV which can be attributed to $LiPF_6$ and LiF, respectively [31–33]. The degradation mechanism for $LiPF_6$ is suggested to be [34]:

$$LiPF_6 \leftrightarrow LiF + PF_5 \quad (3)$$

$$PF_5 + H_2O \leftrightarrow POF_3 + 2HF \quad (4)$$

$$POF_3 + ROH \rightarrow PF_2(OR) + HF \quad (5)$$

$$POF_3 + RCO_3R \rightarrow POF_2OR + CO_2 + RF \quad (6)$$

It is obvious from Fig. 10b that when using VC additive, a larger amount of $LiPF_6$ is found on the SEI, whereas the standard electrolyte exhibits an increased LiF signal. LiBOB and SA additives exhibit an attenuation of the overall F signal compared to both VC and standard electrolyte. Taking the overall F signal into account we find that the $LiPF_6$ content on the SEI of electrodes cycled in electrolyte containing VC is more than three times higher than in LiBOB and SA.

The P 2p spectra (Fig. 10c) show two phosphor species for all cycled electrodes. These two peaks can be assigned to $LiPF_6$ at 136.7 eV and decomposition compounds at 133.5 eV [31–33]. Phosphate has been studied to be the decomposition products on $LiPF_6$-based electrolyte [35,36]. The relative contents of $LiPF_6$ and phosphate are qualitatively in agreement with the data from F 1 s spectra, also supporting the assumption that VC-treated electrodes show the highest amount of $LiPF_6$.

It is seen from Eqs. (3)–(6) that the atomic ratio of the P:F in the products is close to 1:4. However, the atomic ratio of P:F based on XPS analysis (Table 5) is higher. This can be explained by the incomplete washing of the electrolyte.

In summary, XPS provides a quantitative explanation of the processes caused by electrolyte additives and their influence on the batteries' properties in good agreement with the data shown in the previous sections. However, the XPS technique could be completed by Fourier Transform Infrared Spectroscopy (FTIR) to provide a better picture of the SEI.

4. Conclusions

A comparative study was conducted for the Si/MC electrodes with different electrolyte additives: VC, SA, and LiBOB with 5 wt% concentration. The electrochemical tests show that the electrode with VC has an excellent discharge capacity of 1100 mAh g^{-1} for up to 100 cycles. At 1C and 2C, the electrode exhibits a high discharge capacity of 903 mAh g^{-1} and 683 mAh g^{-1}, respectively. The effect of different concentrations of VC was performed. It is shown that increasing the concentration of VC does not improve the electrochemical performance of Si/MC electrodes, which is due to a high content of insulating poly(VC) on the SEI layer. dQ/dV analysis confirms the stability of the electrode with VC 5 wt% by showing no shift of the reduction potential upon cycling. From XPS analysis, it can be concluded that on the electrodes cycled in SA- and LiBOB-containing electrolytes, lithium carbonates are deposited and a thicker SEI layer is formed than with standard and VC-containing electrolyte. In addition, XPS data show that the thinnest SEI layer as well as the highest amount of intact (non-decomposed) $LiPF_6$ is found on the electrode cycled in electrolyte with VC additive.

Acknowledgments

The authors gratefully acknowledge the European Commission for its support of the Marie Curie program through the ITN EMVeM project (GA 315967).

References

[1] J.R. Szczech, S. Jin, Nanostructured silicon for high capacity lithium battery anodes, Energy Environ. Sci. 4 (2011) 56–72.
[2] K. Tasaki, A. Goldberg, M. Winter, On the difference in cycling behaviors of lithium-ion battery cell between the ethylene carbonate- and propylene carbonate-based electrolytes, Electrochim. Acta. 56 (2011) 10424–10435.
[3] K. Xu, Electrolytes and interphasial chemistry in Li ion devices, Energies. 3 (2010) 135–154.
[4] P. Verma, P. Maire, P. Novák, A review of the features and analyses of the solid electrolyte interphase in Li-ion batteries, Electrochim. Acta. 55 (2010) 6332–6341.
[5] J.B. Goodenough, Y. Kim, Challenges for rechargeable Li batteries, Chem. Mater. 22 (2010) 587–603.
[6] S. Dalavi, P. Guduru, B.L. Lucht, Performance Enhancing Electrolyte Additives for Lithium Ion Batteries with Silicon Anodes, J. Electrochem. Soc. 159 (2012) A642–A646.
[7] I.A. Profatilova, C. Stock, A. Schmitz, S. Passerini, M. Winter, Enhanced thermal stability of a lithiated nano-silicon electrode by fluoroethylene carbonate and vinylene carbonate, J. Power Sources. 222 (2013) 140–149.
[8] C.C. Nguyen, B.L. Lucht, Comparative Study of Fluoroethylene Carbonate and Vinylene Carbonate for Silicon Anodes in Lithium Ion Batteries, J. Electrochem. Soc. 161 (2014) A1933–A1938.
[9] L. Martin, H. Martinez, M. Ulldemolins, B. Pecquenard, F. Le Cras, Evolution of the Si electrode/electrolyte interface in lithium batteries characterized by XPS and AFM techniques: The influence of vinylene carbonate additive, Solid State Ionics. 215 (2012) 36–44.
[10] M. Ulldemolins, F. Le Cras, B. Pecquenard, V.P. Phan, L. Martin, H. Martinez, Investigation on the part played by the solid electrolyte interphase on the electrochemical performances of the silicon electrode for lithium-ion batteries, J.Power Sources. 206 (2012) 245–252.
[11] G. Ji, Y. Ma, J.Y. Lee, Mitigating the initial capacity loss (ICL) problem in high-capacity lithium ion battery anode materials, J. Mater. Chem. 21 (2011) 9819–9824.
[12] C. Xu, F. Lindgren, B. Philippe, M. Gorgoi, F. Björefors, K. Edstrom, T. Gustafsson, Improved Performance of Silicon Anode for Li-Ion Batteries: Understanding the Surface Modification Mechanism of Fluoroethylene Carbonate as an Effective Electrolyte Additive, Chem. Mater. 27 (7) (2015) 2591–2599.
[13] X. Chen, X. Li, D. Mei, J. Feng, M.Y. Hu, J. Hu, M. Engelhard, J. Zheng, W. Xu, J. Xiao, J. Liu, J.G. Zhang, Reduction mechanism of fluoroethylene carbonate for stable solid-electrolyte interphase film on silicon anode, ChemSusChem. 7 (2014) 549–554.
[14] M.-Q. Li, M.-Z. Qu, X.-Y. He, Z.-L. Yu, Electrochemical Performance of Si/Graphite/Carbon Composite Electrode in Mixed Electrolytes Containing LiBOB and LiPF, J. Electrochem. Soc. 156 (2009) A294–A298.
[15] G.B. Han, M.H. Ryou, K.Y. Cho, Y.M. Lee, J.K. Park, Effect of succinic anhydride as an electrolyte additive on electrochemical characteristics of silicon thin-film electrode, J. Power Sources. 195 (2010) 3709–3714.

[16] Y. Li, G. Xu, Y. Yao, L. Xue, S. Zhang, Y. Lu, O. Toprakci, X. Zhang, Improvement of cyclability of silicon-containing carbon nanofiber anodes for lithium-ion batteries by employing succinic anhydride as an electrolyte additive, J. Solid State Electrochem. 17 (2013) 1393–1399.
[17] G.-B. Han, J.-N. Lee, J.W. Choi, J.-K. Park, Tris(pentafluorophenyl) borane as an electrolyte additive for high performance silicon thin film electrodes in lithium ion batteries, Electrochim. Acta. 56 (2011) 8997–9003.
[18] A. Rezqita, R. Hamid, S. Schwarz, H. Kronberger, A. Trifonova, Conductive Additive for Si/Mesoporous Carbon Anode for Li-Ion Batteries: Commercial Graphite vs Super C65, ECS Trans. 66 (2015) 17–27.
[19] S. Tougaard, Universality Classes of Inelastic Electron Scattering Cross-sections, Surf. Interface Anal. 25 (1997) 137–154.
[20] J.H. Scofield, Hartree-Slater subshell photoionization cross-sections at 1254 and 1487 eV, J. Electron Spectros. Relat. Phenomena. 8 (1976) 129–137, doi: http://dx.doi.org/10.1016/0368-2048(76)80015-1.
[21] N.S. Choi, K.H. Yew, H. Kim, S.S. Kim, W.U. Choi, Surface layer formed on silicon thin-film electrode in lithium bis(oxalato) borate-based electrolyte, J. Power Sources. 172 (2007) 404–409.
[22] T.H. Hwang, Y.M. Lee, B.-S. Kong, J.-S. Seo, J.W. Choi, Electrospun core-shell fibers for robust silicon nanoparticle-based lithium ion battery anodes, Nano Lett. 12 (2012) 802–807.
[23] K.W. Schroder, J. Alvarado, T.A. Yersak, J. Li, N. Dudney, L.J. Webb, Y.S. Meng, K.J. Stevenson, The Effect of Fluoroethylene Carbonate as an Additive on the Solid Electrolyte Interphase on Silicon Lithium-ion Electrodes, Chem. Mater. 27 (16) (2015) 5531–5542.
[24] K. Xu, S.S. Zhang, U. Lee, J.L. Allen, T.R. Jow, LiBOB. Is it an alternative salt for lithium ion chemistry? J. Power Sources. 146 (2005) 79–85.
[25] M.N. Obrovac, L.J. Krause, Reversible Cycling of Crystalline Silicon Powder, J. Electrochem. Soc. 154 (2007) A103–A108.
[26] V.L. Chevrier, L. Liu, D.B. Le, J. Lund, B. Molla, K. Reimer, L.J. Krause, L.D. Jensen, E. Figgemeier, K.W. Eberman, Evaluating Si-Based Materials for Li-Ion Batteries in Commercially Relevant Negative Electrodes, J. Electrochem. Soc. 161 (2014) A783–A791.
[27] X. Zhang, R. Kostecki, T.J. Richardson, J.K. Pugh, P.N. Ross, Electrochemical and infrared studies of the reduction of organic carbonates, J. Electrochem. Soc. 148 (2001) A1341–A1345.
[28] R. Hausbrand, G. Cherkashinin, H. Ehrenberg, M. Gröting, K. Albe, C. Hess, W. Jaegermann, Fundamental degradation mechanisms of layered oxide Li-ion battery cathode materials: Methodology insights and novel approaches, Mater. Sci. Eng. B Solid-State Mater. Adv. Technol. 192 (2015) 3–25.
[29] G. Beamson, D. Briggs, High Resolution XPS of Organic Polymers The Scienta ESCA300 Database, Wiley, 1992.
[30] R. Dedryvère, L. Gireaud, S. Grugeon, S. Laruelle, J.M. Tarascon, D. Gonbeau, Characterization of lithium alkyl carbonates by X-ray photoelectron spectroscopy: Experimental and theoretical study, J. Phys. Chem. B. 109 (2005) 15868–15875.
[31] R. Dedryvère, S. Laruelle, S. Grugeon, L. Gireaud, J.-M. Tarascon, D. Gonbeau, XPS Identification of the Organic and Inorganic Components of the Electrode/Electrolyte Interface Formed on a Metallic Cathode, J. Electrochem. Soc. 152 (2005) A689–A696.
[32] Y.-C. Yen, S.-C. Chao, H.-C. Wu, N.-L. Wu, Study on Solid-Electrolyte-Interphase of Si and C-Coated Si Electrodes in Lithium Cells, J. Electrochem. Soc. 156 (2009) A95–A102.
[33] B. Philippe, M. Hahlin, K. Edstro m, T. Gustafsson, H. Siegbahn, H. Rensmo, Photoelectron Spectroscopy for Lithium Battery Interface Studies, J. Electrochem. Soc. 163 (2015) A178–A191.
[34] D. Aurbach, B. Markovsky, A. Shechter, Y. Ein-Eli, A Comparative Study of Synthetic Graphite and Li Electrodes in Electrolyte Solutions Based on Ethylene Carbonate-Dimethyl Carbonate Mixtures, J. Electrochem. Soc. 143 (1996) 3809–3820.
[35] A. Guéguen, D. Streich, M. He, M. Mendez, F.F. Chesneau, P. Novák, E.J. Berg, Decomposition of LiPF 6 in High Energy Lithium-Ion Batteries Studied with Online Electrochemical Mass Spectrometry, J. Electrochem. Soc. 163 (2016) A1095–A1100.
[36] A.M. Andersson, D.P. Abraham, R. Haasch, S. MacLaren, J. Liu, K. Amine, Surface Characterization of Electrodes from High Power Lithium-Ion Batteries, J. Electrochem. Soc. 149 (2002) A1358–A1369.